Electronic Supplementary Information

Dual non-covalent bonding constructed continuous interfacial structure for reducing interfacial thermal resistance

Bin Wu, [‡,*a] Ya Li, [‡,a] Wei Chen, [b] Boyang Ding, [a] Peng Chen,[a] Ru Xia [a] and Jiasheng Qian*[a]

[a]Key Laboratory of Environment-Friendly Polymeric Materials of Anhui Province, School of Chemistry & Chemical Engineering, Anhui University, Hefei, Anhui, 230601, China

[b]School of Materials and Chemical Engineering, Anhui Jianzhu University, Hefei, Anhui, 230009, China

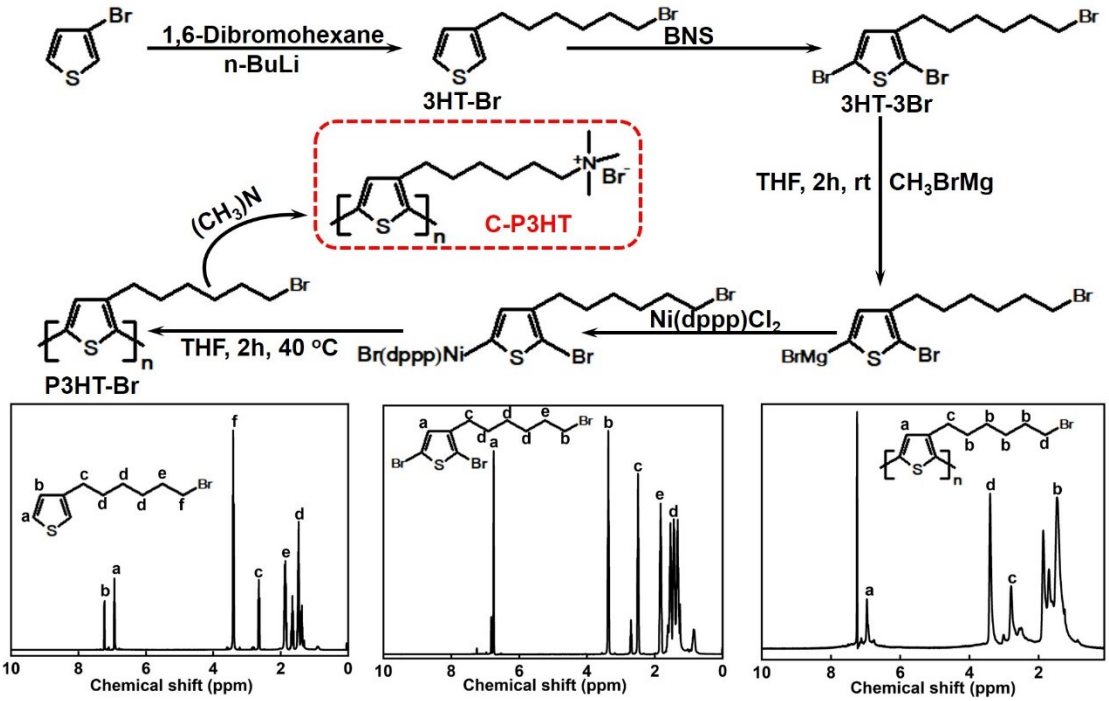

Fig. S1 The flow-chart of preparation route of C-P3HT and corresponding ^{1}H NMR spectrum.

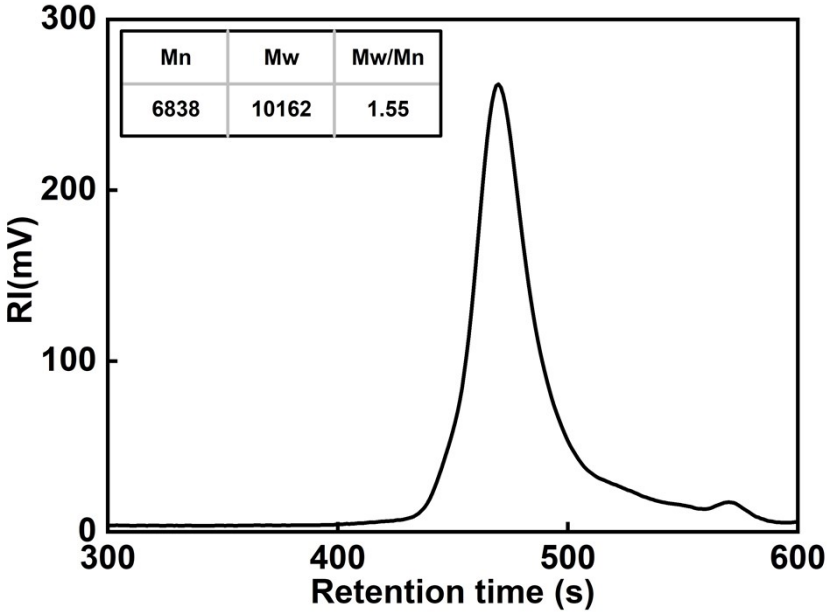

Fig. S2 GPC of P3HT-Br.

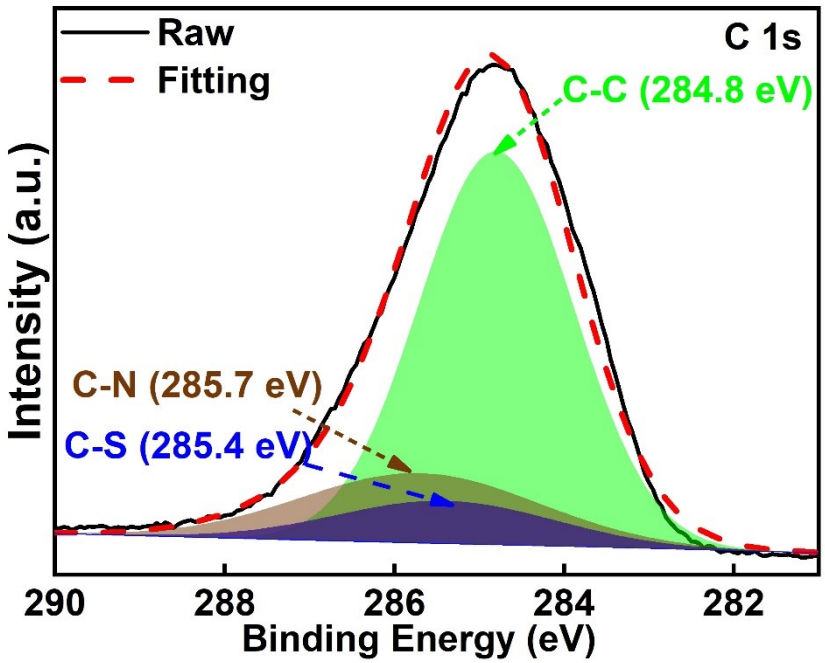

Fig. S3 XPS of C-P3HT.

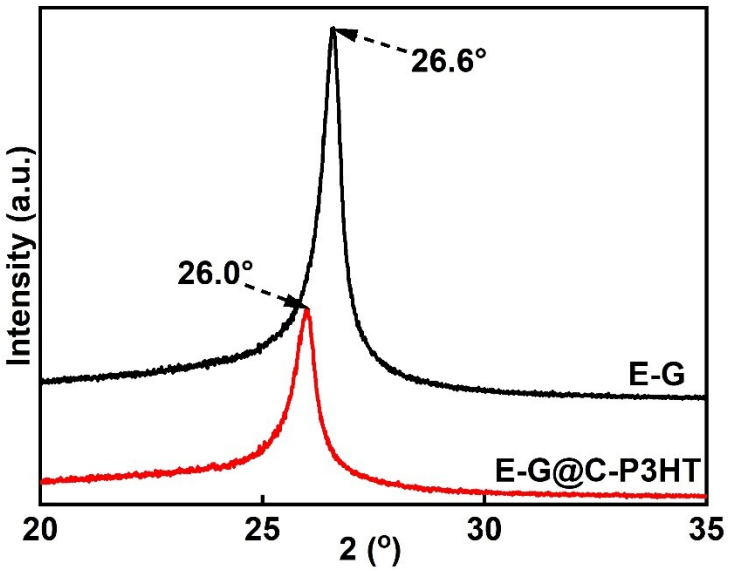

Fig. S4 The XRD of E-G and E-G@C-P3HT.

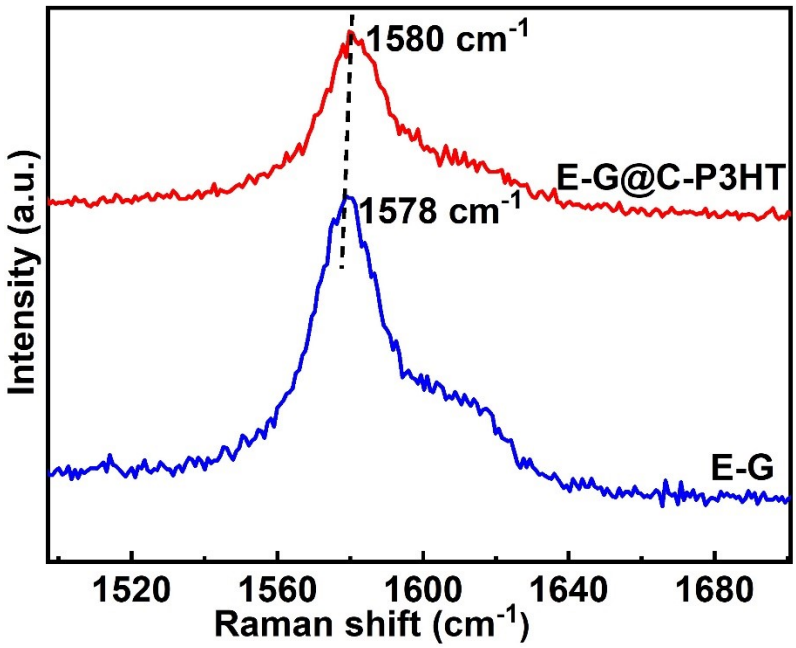

Fig. S5 Raman spectra of E-G and E-G@C-P3HT.

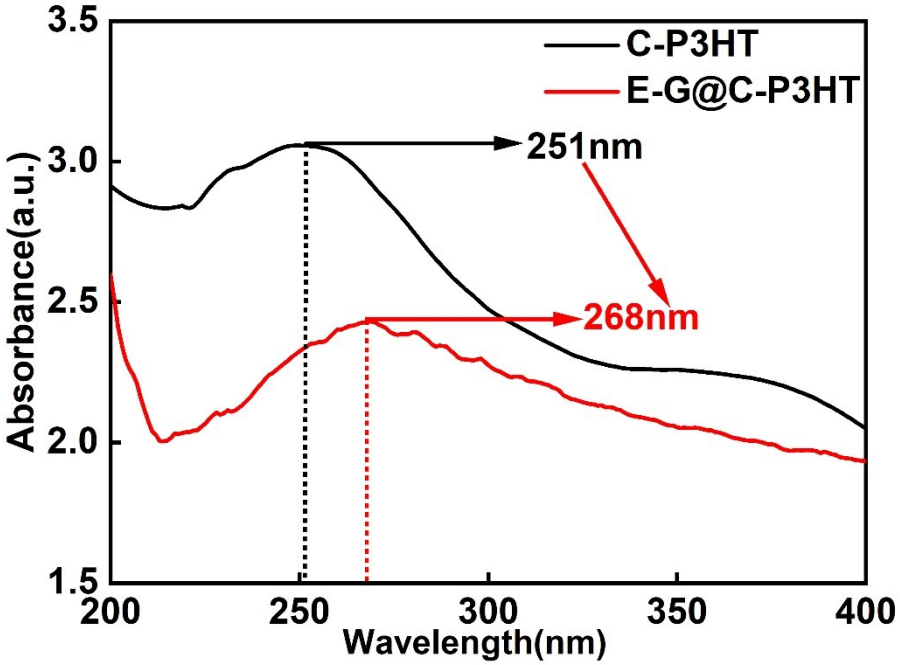

Fig. S6 UV/Vis absorption spectra of C-P3HT and E-G@ C-P3HT.

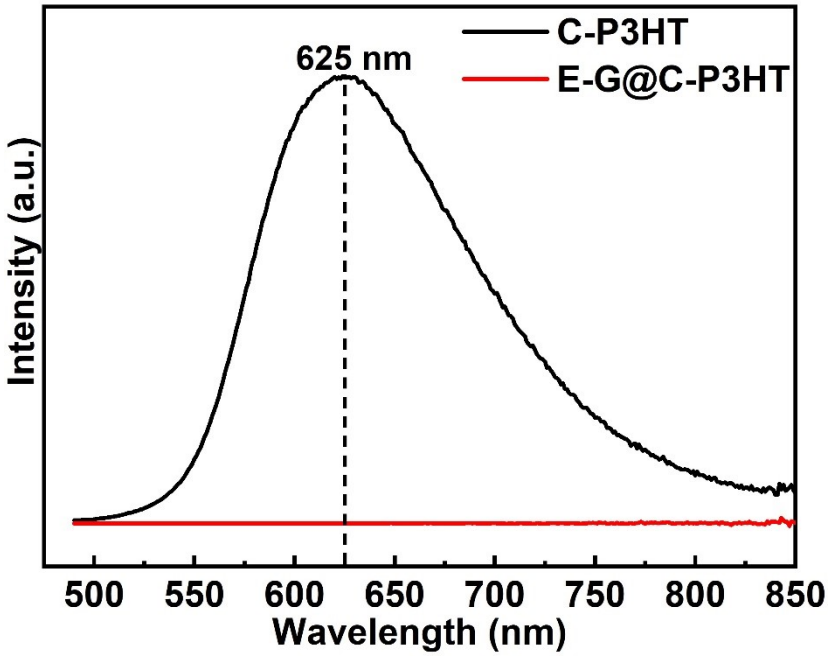

Fig. S7 Fluorescence spectra (λ=470 nm) of C-P3HT (0.1 mg/mL) and E-G@ C-P3HT in water.

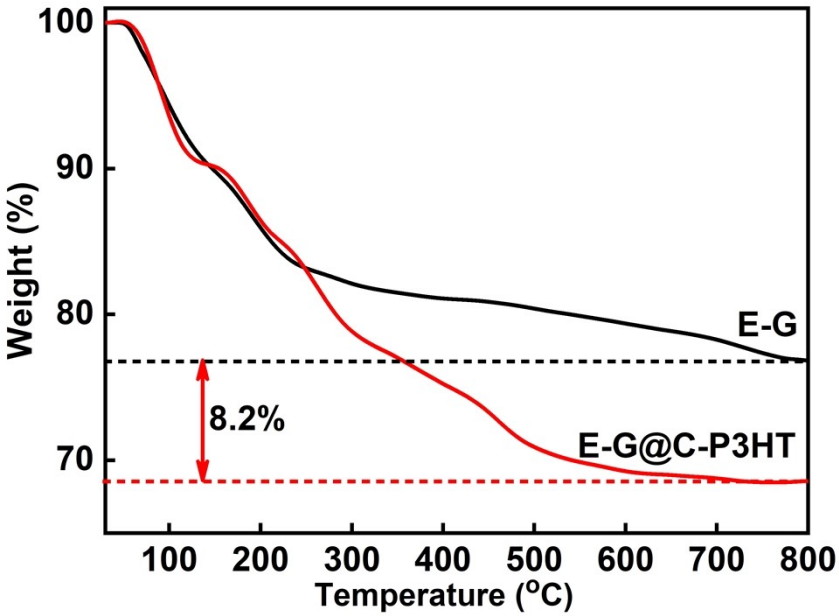

Fig.S8 TGA of E-G and E-G@CP3HT.

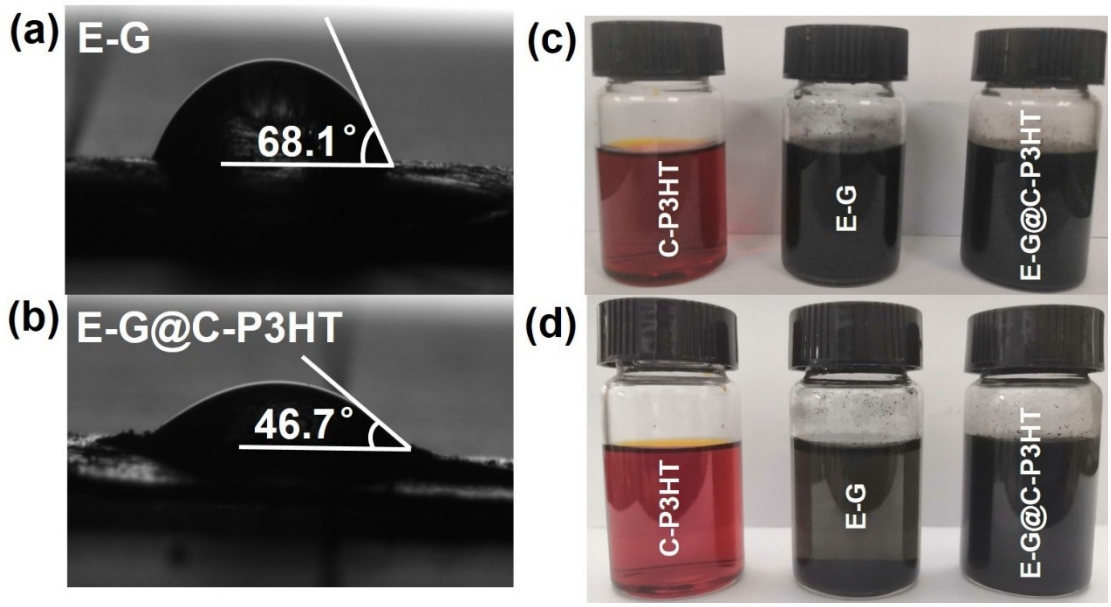

Fig. S9 (a~b) Contact angle measurements of E-G and E-G@C-P3HT. Optical image of C-P3HT, E-G and E-G@C-P3HT in water (c) before and (d) after storage for 10 days.

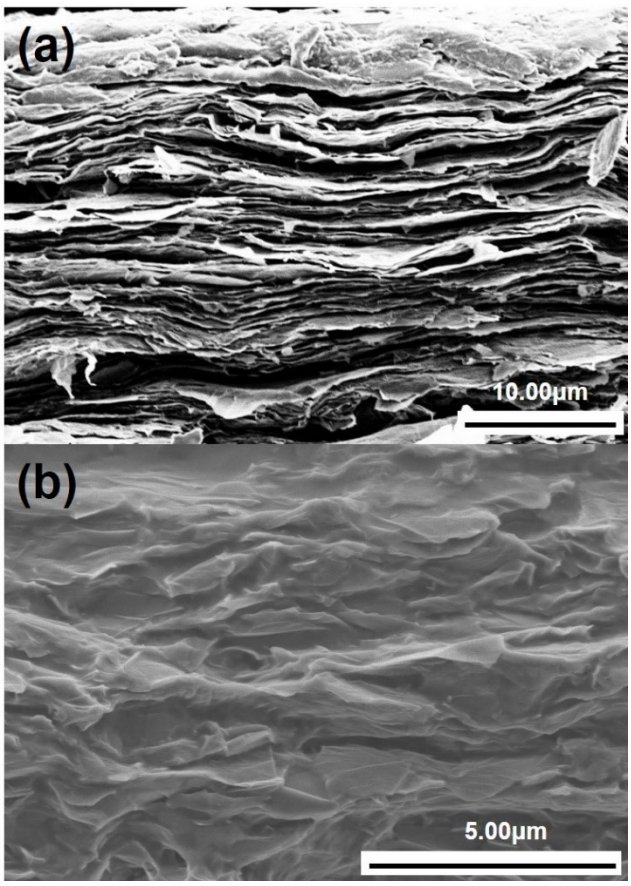

Fig. S10 SEM cross-section images of (a) E-G/PVA and (b) E-G@C-P3HT/PVA with 15wt% filler loading.

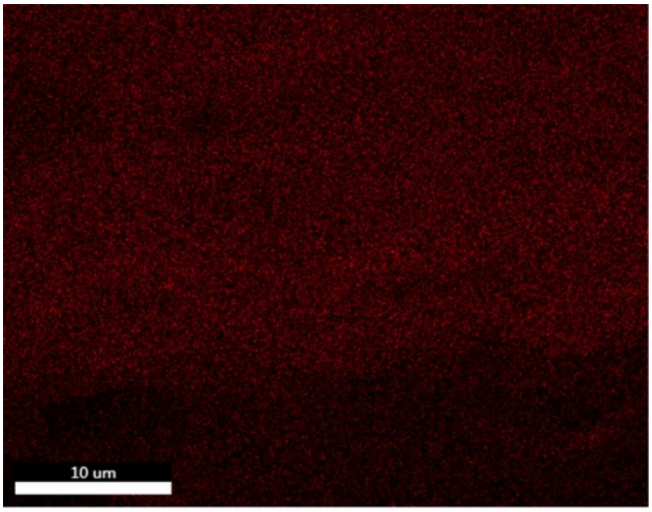

Fig. S11 Sulfur elemental mapping image of E-G@C-P3HT.

As E-G was the main thermal conductivity filler, it is necessary to analyze the interface thermal resistance (R_i) between E-G layersin detail before and after C-P3HT modification. The nonlinear model proposed by Foygel et al. to calculate the interfacial thermal resistance [1-3]. The model is given by the following equations.

$$\kappa_c-\kappa_m = \kappa_0[(V_f- V_c)/(1- V_c)]^\tau \quad (1)$$

where κ_c and κ_m are the thermal conductivity of the composites with different filler loading and PVA, respectively. κ_0 is a pre-exponential factor ratio associated with contribution of filler. V_f is the volume fraction of fillers in composites. V_c is the key volume content of filler related to percolation threshold of thermal conductivity. As depicted in Fig. S12, the V_c values are 0.73 vol% and 0.75vol% for the E-G/PVA and E-G@C-P3HT/PVA, respectively. τ is a heat transfer exponent dependent on the aspect ratio of filler.

To calculate the R_i between filler, we have transformed the Foygel model formula as follows.

$$\kappa_c-\kappa_m = \kappa_0[(V_f- V_c)/(1- V_c)]^\tau \quad (2)$$

$$\lg(\kappa_c-\kappa_m) = \lg\{\kappa_0[(V_f- V_c)/(1- V_c)]^\tau\} \quad (3)$$

$$\lg(\kappa_c-\kappa_m) = \lg\kappa_0 + \tau\lg[(V_f - V_c)/(1 - V_c)] \quad (4)$$

The formula can be simplified as:

$$y=a+bx \quad (5)$$

where y equals to $\lg(\kappa_c-\kappa_m)$, x equals to $\lg[(V_f - V_c)/(1 - V_c)]$, a equals to $\lg k_0$ and b equals to τ. As shown in Fig.S13, the slope and intercept of the fitted line correspond to τ and $\lg k_0$. And the calculated k_0 and τ of E-G/PVA and E-G@C-P3HT/PVA were exhibited in Table. S1.

The contact resistance (R) between E-G layers or between E-G@C-P3HT can be found according to the equation.

$$R = 1/(\kappa_0 L V_c^\tau) \quad (6)$$

where L is the sheet size of the filler. The distribution of E-G and E-G@C-P3HT sheet size were obtained by dynamic light scattering in Fig. S14. The mean sheet size of E-G and E-G@C-P3HT was 4150 and 4800 nm. The calculated R values are 2.30×10^5 K W^{-1} and 0.53×10^5 K W^{-1} for the E-G/PVA and E-G@C-P3HT/PVA, respectively.

The interface thermal resistance (R_i) between E-G layers or between E-G@C-P3HT was obtained by following the equation.

$$R_i=R\times S_c \quad (7)$$

where S_c is the average overlap area between E-G or between E-G@C-P3HT. Considering the reassembly of E-G or E-G@C-P3HT during the vacuum-assisted filtration, it is more proper to calculate S_c using the size of 2D nanofillers in the composites. It can be assumed that 1/100 of each E-G or E-G@C-P3HT is involved in the heat conduction of network[1]. Therefore, S_c of E-G and E-G@C-P3HT was 1.35×10^{-13} m^2 and 1.81×10^{-13} m^2, respectively.

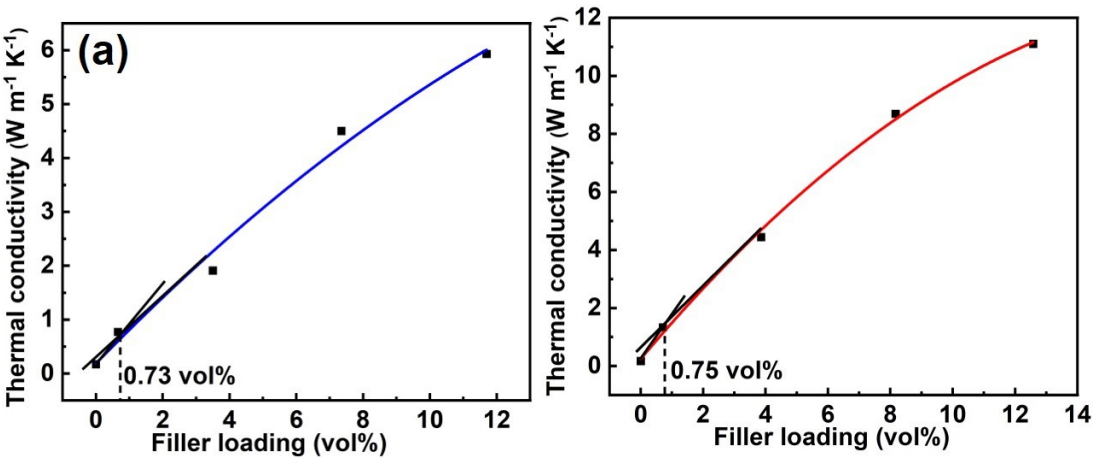

Fig. S12 V_c achieved by tangential process of experimental data for (a) E-G and (b)E-G@C-P3HT.

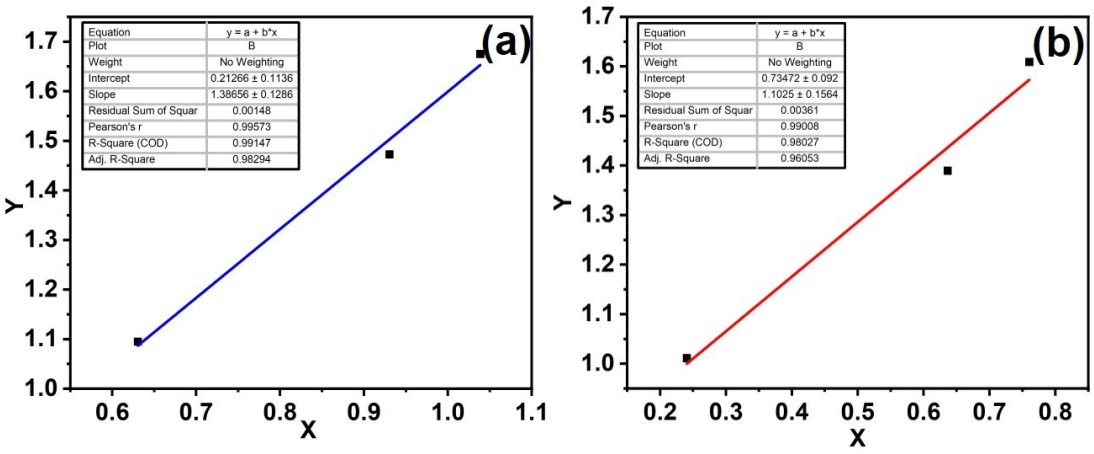

Fig. S13 The fitting process of Foygel model for (a) E-G/PVA and (b) E-G@C-P3HT/PVA.

Table S1. k_0 and τ in Foygel model for E-G/PVA and E-G@C-P3HT/PVA.

Sample	k_0(W m^{-1} K^{-1})	τ
E-G/PVA	1.62	1.39
E-G@C-P3HT/PVA	5.37	1.10

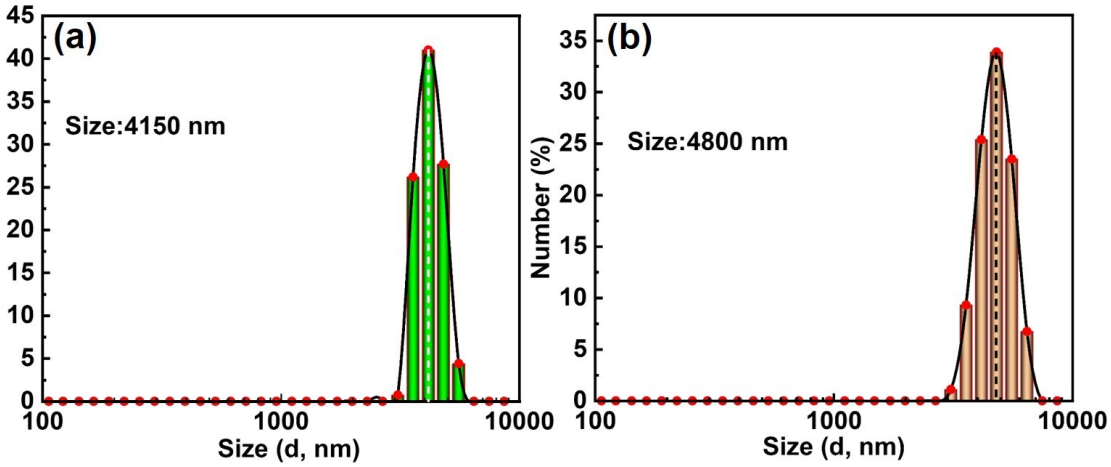

Fig. S14 The distribution of sheet size of E-G and E-G@C-P3HT obtained by dynamic light scattering, respectively.

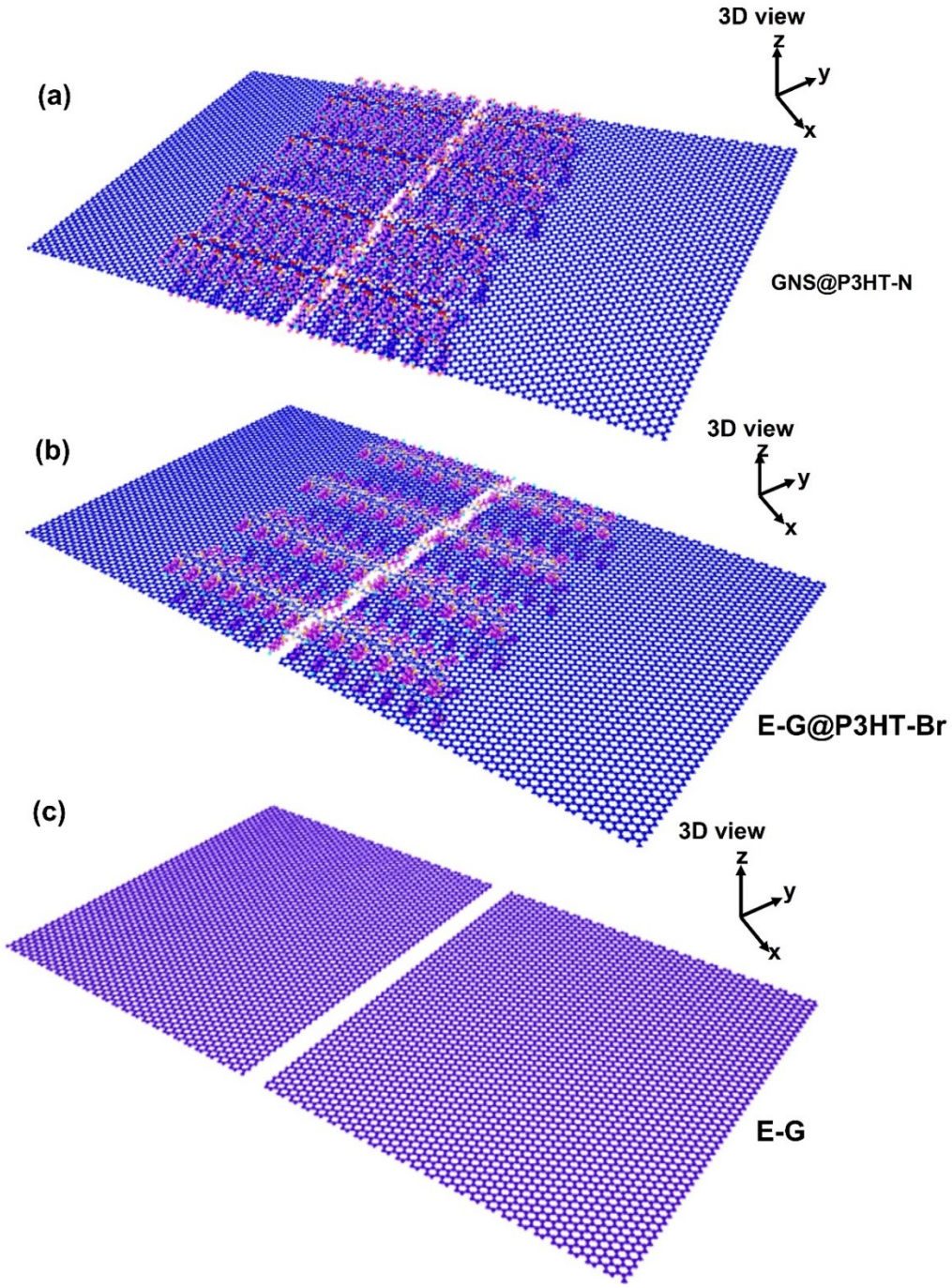

Fig. S15 Simulation modeling of E-G@C-P3HT, E-G@ P3HT-Br, and E-G, respectively.

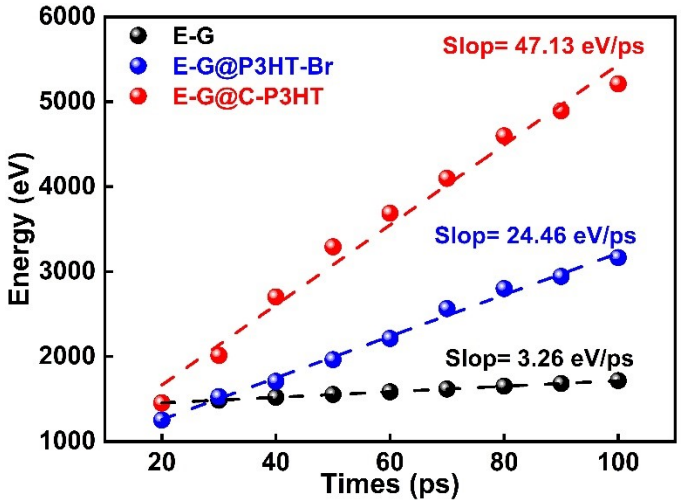

Fig. S16 Accumulated thermal energy as a function of the time in steady state for E-G@C-P3HT, E-G@ P3HT-Br, and E-G.

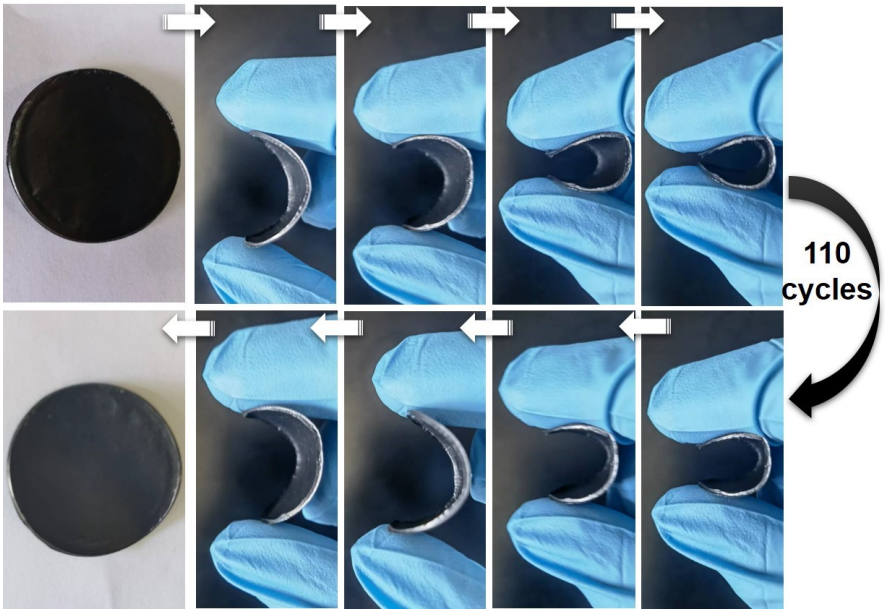

Fig. S17 corresponding variations of morphology as functions of bending cycles.

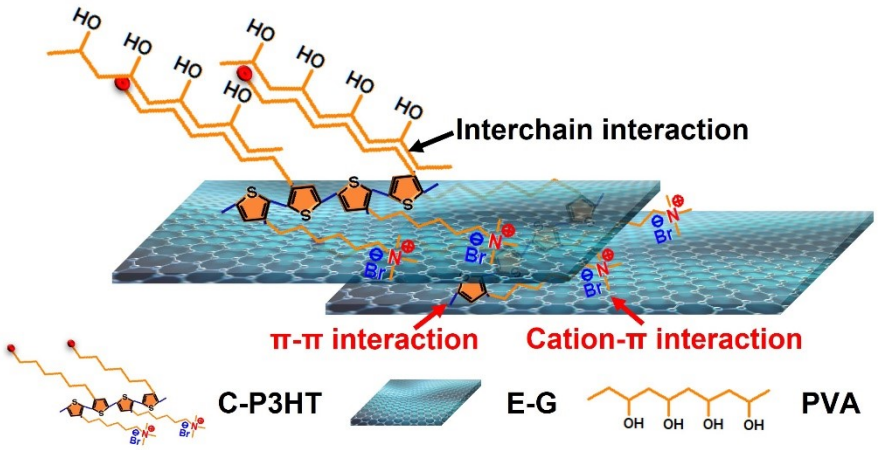

Fig. 18 Schematic illustration of non-covalent bonding interaction between E-G layers and between E-G and PVA by C-P3HT modification.

Reference

1. Y. Yao, J. Sun, X. Zeng, R. Sun, J. B. Xu and C. P. Wong, *Small*, 2018, **14**, 1704044.
2. Z. G. Wang, M. Z. Chen, Y. H. Liu, H. J. Duan, L. Xu, L. Zhou, J. Z. Xu, J. Lei and Z. M. Li, *J. Mater. Chem. C*, 2019, **7**, 9018-9024.
3. Y. Zhang, C. Lei, K. Wu and Q. Fu, *Adv. Sci.*, 2021, **8**, 2004821.